

PAPER • OPEN ACCESS

Near-surface elevated pollution: what we don't know doesn't hurt? A numerical study over Mt. Carmel

To cite this article: Nitsa Haikin and Pinhas Alpert 2019 *Environ. Res. Commun.* **1** 085003

View the [article online](#) for updates and enhancements.

Environmental Research Communications



PAPER

Near-surface elevated pollution: what we don't know doesn't hurt? A numerical study over Mt. Carmel

OPEN ACCESS

RECEIVED
23 April 2019REVISED
22 July 2019ACCEPTED FOR PUBLICATION
1 August 2019PUBLISHED
22 August 2019

Original content from this work may be used under the terms of the [Creative Commons Attribution 3.0 licence](#).

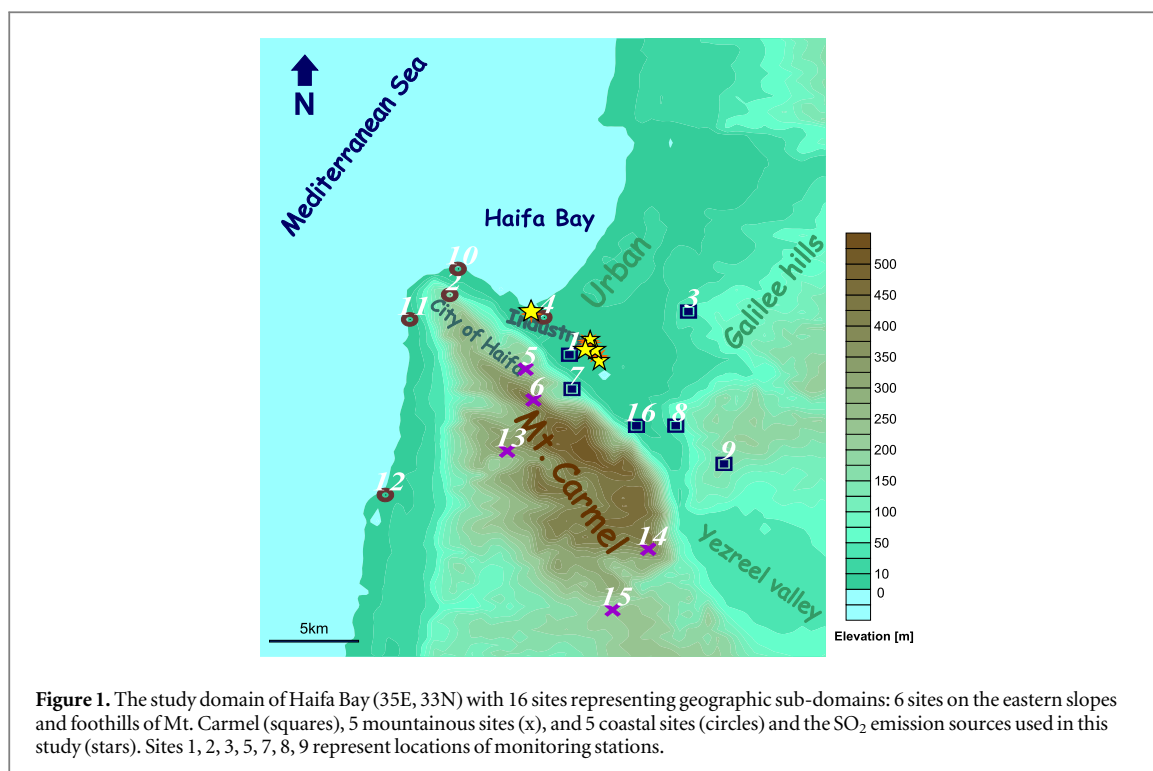
Any further distribution of this work must maintain attribution to the author(s) and the title of the work, journal citation and DOI.

Nitsa Haikin^{1,2} and Pinhas Alpert¹ ¹ Department of Geophysics, Faculty of Exact Sciences, Tel-Aviv University, Tel-Aviv 69978, Israel² Department of Physics, NRCN, POB 9001, Beer-Sheba 84190, IsraelE-mail: nitsahai@tauex.tau.ac.il**Keywords:** air pollution, atmospheric modeling, elevated pollution layers, inversionSupplementary material for this article is available [online](#)**Abstract**

Many air pollution events are occasionally difficult to explain. While most monitoring-based air pollution assessment studies deal with surface analysis, the near-surface elevated pollutants are challenging. The lack of data and understanding of those elevated layers, leaves us 'blind' and with no clue where, when and how intensively these pollutants may hit the surface. Here, this challenge at the specific domain of Mt. Carmel is addressed. The atmospheric numerical models RAMS and HYPACT were employed on Haifa Bay in the Eastern Mediterranean with nested horizontal grids down to 0.5 km, in order to resolve the fine-scale flow, along an air pollution episode which serves as a case study. Sixteen locations were determined, representing monitored and non-monitored sites in the complex terrain sub-domains. Results show multi-inversion profiles, which are consistent with an earlier observational study over the region. Concentration differences up to an order of magnitude between adjacent sites (~2 km) were found, often associated with near-zero surface values, while some simulated peaks were at elevations of 100–400 m above ground level (AGL). The current event offers a view on the near-surface elevated layers, and points at limitations of ground-level monitoring as an indicator of air pollution. This study highlights the importance of near-surface pollution, which is often an unknown source for surface pollution. Overall, steep vertical gradient of pollution as shown here is associated with a combination of deep inversion (or multi-inversion profile), vertical circulation due to topography or synoptic flow, and small scale circulation induced by the complex topography. Since monitoring of the elevated layers is limited by the technology, it is suggested that high resolution advanced models should be used for further exploration of the near-surface pollution.

1. Introduction

Air pollution episodes strongly depend on synoptic to local scale meteorological conditions (e.g., Kallos *et al* 1993, Astitha *et al* 2008, Matthaios *et al* 2017), and may occur either in the vicinity of emission sources or farther away. Most pollutants that are emitted into the boundary layer remain and disperse within it, and may occasionally be caught and accumulated under a strong or long-lived inversion layer (Stull 1988, Kotroni *et al* 1999). However, some pollutants may be emitted above the capping inversion and/or be transported to higher layers where they may accumulate and persist, especially in coastal areas where diurnal mesoscale circulation dominates (e.g., Soriano *et al* 2001). Coastal mesoscale recirculation of sea-land breeze may also cause accumulation of air pollutants due to plumes return flow, as was found at the Israeli Mediterranean coast by Alper-Siman-Tov *et al* (1997) and Levy *et al* (2009). Simulated mountainous coastline flow suggest that sea breeze and topographic forcing produce a more intense circulation when combined (e.g., Mahrer and Pielke 1977, Perez-Landa *et al* 2007). Such circulations could be suggested as another mechanism for a buildup of high concentrations in some locations. Slope flows and convergence zones in complex terrain may also induce significant vertical and circular transport of pollutants (e.g., Lang *et al* 2015, Wagner *et al* 2015). Reuten *et al* (2004) observed slope flow in the convective



boundary layer (CBL), and their calculated mass transport suggested a closed slope-flow circulation within the CBL, in which air pollutants may be trapped.

Atmospheric modeling over complex terrain requires adequate resolution in order to represent a realistic and accurate flow. Studies of air pollution in regions of complex terrain achieved improved accuracy and were able to better explain local flow and pollution dispersion when high resolution (1–4 km) models were employed (e.g., Grell *et al* 2000, Jazcilevich *et al* 2003, Schmitz 2005, Ritter *et al* 2013, Valverde *et al* 2016). High resolution modeling allows effective and realistic comparison between simulation results and local ground monitoring sites within the study domain (e.g., Perez-Landa *et al* 2007, Balanzino and Trini Castelli 2018), which is also important for an efficient model validation. In this study the numerical atmospheric models RAMS and HYPACT were employed with high resolution (0.5 km) to resolve spatial and temporal patterns in the fine-scale complex domain of Haifa, addressing the pollution dispersion within the near-surface elevated layers. The Haifa region in northern Israel is characterized by a complex terrain on the Mediterranean coast (figure 1). Previous air pollution studies over the Haifa basin addressed health effects (Goren *et al* 1990, Paz *et al* 2009, Eitan *et al* 2010), identification and analysis of pollutants (Mamane and Mehler 1987, Mamane and Gottlieb 1995, Garty *et al* 2001), two-dimensional analysis based on monitoring data (Yuval and Broday 2006, Eitan *et al* 2010), and modeling of potential SO₂ concentrations (Doron and Kinrot 1989). Although Haifa densely populated area is relatively quite well-covered by monitoring stations (about 1 monitoring station for every 20 km²), there are flow patterns which the observations are insufficient to capture (e.g. Pielke *et al* 1983). Most air pollution assessments are based on surface data (e.g. Kerr and Waugh 2018, McLagan *et al* 2018) and do not refer to the elevated layers. This may be justified by the focus on population exposure. A minority of the reported studies regard elevated air pollution modeling in complex terrain (e.g. Matthaïos *et al* 2017b), and some refer to pollutants concentrations in (indoor and outdoor) urban high-building environment (e.g. Sajani *et al* 2018).

Here, we focus on some major variability between the pollution patterns at the surface and at elevated layers, over the Haifa complex domain. An air pollution episode was chosen as a case study to challenge the question whether it is justified to ignore near-surface elevated pollution. The mesoscale flow over the domain was investigated with a focus on the pollutants dispersion at surface and near-surface levels. The prevailing synoptic system along the event was a Red Sea Trough with easterly flow in the region, which expectedly would result with low pollution concentrations over the study domain due to the off-shore flow. However, at that specific day, high concentrations of SO₂ were recorded in a few monitoring stations. The formation mechanism and the timing of the peak concentrations could not be explained by the ground observations alone, and atmospheric numerical modeling was employed for exploration of the event. The atmospheric conditions, the pollutant sources and receptors, and model description are given in section 2; local flow patterns with selected upper-air analysis are discussed in section 3.

2. Data and methodology

Following are descriptions of the domain characteristics (section 2.1), the numerical model (section 2.2), and the emission sources and receptors which were used in this study (sections 2.3, 2.4, respectively).

2.1. Regional characteristics

The Haifa region in northern Israel is characterized by a complex terrain adjacent to the Mediterranean Sea, with Mt. Carmel ridge rising from the coastline up to an altitude of 450–500 m (ASL). Haifa Bay (35.1E, 32.5N) is bordered by easterly hills 10 km away from the coastline and the north-easterly Upper Galilee summits of 600–1200 m, 20 km away. The city of Haifa is spread over the ridge, and a few densely populated towns are located on the coastal plain of the bay, adjacent to industrial zones (figure 1).

2.2. Numerical models

2.2.1. RAMS

The numerical Regional Atmospheric Modeling System RAMS 6.0 (Cotton *et al* 2003) was employed with four nested grids from synoptic to fine-scale resolution (32, 8, 2, 0.5 km). A total of 42 vertical layers were defined, from 50 m AGL up to 20 km, out of which 11 levels are within the lower 1 km of the troposphere, hereby referred by rounded values (105 rounded to 100 m, etc). RAMS was initiated with 2.5° NCEP reanalysis data (Kalney 1996) and updated every 6 hr. RAMS simulation results were used as an input to the HYPACT simulation.

2.2.2. HYPACT

The HYbrid PArticle and Concentration Transport Model HYPACT (Walko *et al* 2001) version 1.9 was employed in the current study. HYPACT simulations were employed on the inner grid of RAMS, at a domain size of 60 km × 60 km. Emissions of SO₂ from the largest emission sources were simulated from 0100 UTC to 2200 UTC, with steady continuous emissions. No pollutant removal from the plume was included. The results were extracted in a 10 min time resolution.

2.3. Emission sources

The SO₂ pollutant was chosen as a tracer for this study, due to well established database of emission sources and ambient monitoring of this pollutant in the region. Emission data was obtained from the Ministry of the Environment, based on their 2006 inventory. Emission rates of the largest SO₂ sources in the region were used, and steady continuous emission rates were assumed. No pollutant removal from the plume was considered, since SO₂ residence time in the troposphere is in the range of a day (Hobbs 2000), while the simulation lasts hours.

2.4. Observations and simulation receptors

About 20 monitoring stations are spread over the region, out of which seven major sites were chosen for this study. Sixteen receptors were defined for the simulation, representing the different geographic sub-domains: the eastern foothills of Mt. Carmel (1, 3, 7, 8, 9, 16), the ridge top and slopes (5, 6, 13, 14, 15), and the coastal zone (2, 4, 10, 11, 12 in figure 1). Seven of the receptors represent locations of the monitoring stations (1, 2, 3, 5, 7, 8, 9 in figure 1), while the others are located at non-monitored sites. In the following section 3 simulation results at these receptors are discussed.

3. Results and discussion

The numerical simulation provided spatial information of the flow and dispersion patterns along the event. Here the prevailing synoptic system along the event is described in section 3.1, mesoscale and local atmospheric patterns are presented in section 3.2, and selected near-surface profiles of pollutants are discussed in section 3.3.

3.1. Synoptic sea-level pressure system

The dominating synoptic system was a low pressure penetration from the Red Sea towards the Eastern Mediterranean coast, called a Red Sea Trough (RST) with a central axis over Israel (figure 2(a)). Such a system forces easterly to north-westerly winds over the Haifa domain. The RAMS simulated synoptic flow shows similar pressure gradient, however, with more of an eastern RST (figure 2(b)), in which case the pressure gradient forces more northerly to north-westerly winds in the domain ('central' or 'eastern axis' refer to the axis position relative to Israel). The RST incidence over Israel is about 9% (based on Alpert *et al* 2004), mostly occurs in spring or fall.

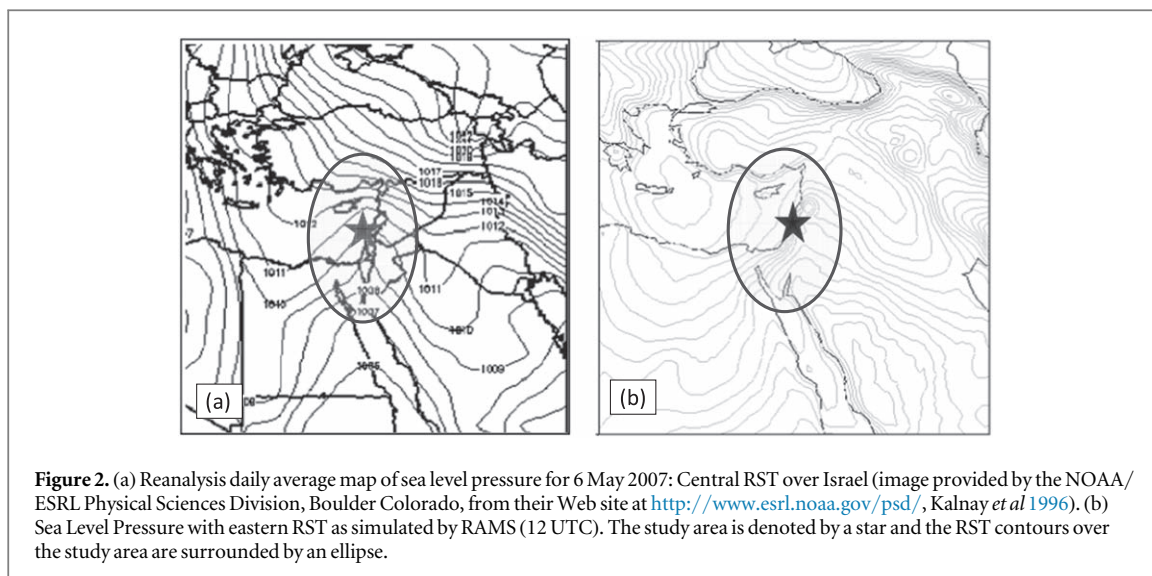


Figure 2. (a) Reanalysis daily average map of sea level pressure for 6 May 2007: Central RST over Israel (image provided by the NOAA/ESRL Physical Sciences Division, Boulder Colorado, from their Web site at <http://www.esrl.noaa.gov/psd/>, Kalnay *et al* 1996). (b) Sea Level Pressure with eastern RST as simulated by RAMS (12 UTC). The study area is denoted by a star and the RST contours over the study area are surrounded by an ellipse.

3.2. Mesoscale and local atmospheric features

The atmospheric flow on 6 May 2007 started as easterly synoptic flow from ground to about 2.5 km AGL and higher. Easterly flow in this region is continental and causes a transport of the largest plumes towards the sea. The model showed a development of deep east-west vertical circulation along the day, which resulted with the near surface wind turning into westerly. Flow patterns such as horizontal and vertical local-scale circulations were identified, apparently affecting the pollution dynamics at surface and at near-surface elevated layers. A brief discussion on the simulated surface flow is presented in the next section 3.2.1, and selected simulated multi-inversion thermal profiles are discussed next (section 3.2.2).

3.2.1. Surface flow pattern

Under the easterly synoptic flow, the simulated morning surface flow over Haifa Bay shows off-shore horizontal circulation cells of 10–20 km diameter within Mt. Carmel wake zone, as demonstrated in figure 3. The local wind direction associated with the evolution of the off-shore cells is generally easterly over the ridge and south-easterly below the northern slopes of Mt. Carmel. These circulation cells must have served as pollutant trap, as corroborated by peak SO_2 concentrations of 400 and $700 \mu\text{g m}^{-3}$ in near-surface elevated layers above sites 10 and 2 respectively (figure 5). These circulation cells disappear when the coastal flow veer into northerly flow (figure 3, 1000 UTC).

Surface concentrations were extracted from the simulation results for eight receptors over the domain, and compared with observations from six sites (1, 3, 5, 7, 8, 9 as in figure 1). Receptors 4 and 16 were set for this study at non-monitored sites, while all the others represent monitoring stations in the domain. Maximum half-hourly values of $300\text{--}400 \mu\text{g m}^{-3} \text{SO}_2$ were recorded along the study day, an order of magnitude higher than the background level. The maximum observed values were compared with the simulated maxima and they showed a fairly similar pattern (figure 4). Then, for each sub-period of the day (based on the peaks pattern) we verified which receptor presented the most significant concentrations, as an indicator of the pollution plume. We compared and concluded the deviation of the simulated from observed ground level indicators. We found that the simulation receptors 4 and 16 had a significant impact, suggesting these locations are unique in terms of spatial distribution of pollutants in the domain. At the Carmel foothills we found sideways deviation (Site 8 versus 16 or 9), vertical deviation (site 5 versus 7) and even significant downwind deviation (namely site 9 versus 4). These results are summed in table S1 and available online at stacks.iop.org/ERC/1/085003/mmedia. The deviations between the indicators may hint at the uncertainty of the simulation, or the uncertainty of the plume location.

3.2.2. Near-surface stable layers

The Haifa region is subjected to multi-inversion thermal profiles, due to topographic effects, mesoscale marine or subsidence inversions, and radiation inversions. Each inversion layer may have a different inner-structure and life-time, some break into sub layers, as presented by Haikin *et al* (2015). In general, the simulated thermal profiles in this case study are multi-inversion and show surface and near-surface inversion layers throughout the day. During most of that day, the temperature at 0.6 km ASL remains higher than at surface, associated with strong inversion beneath. The deepest and strongest inversions were found over the bay and the coastal sites, some as strong as 10 to $12 \text{ K (100 m)}^{-1}$ (figure 5). It is assumed that the relationship between the type of the

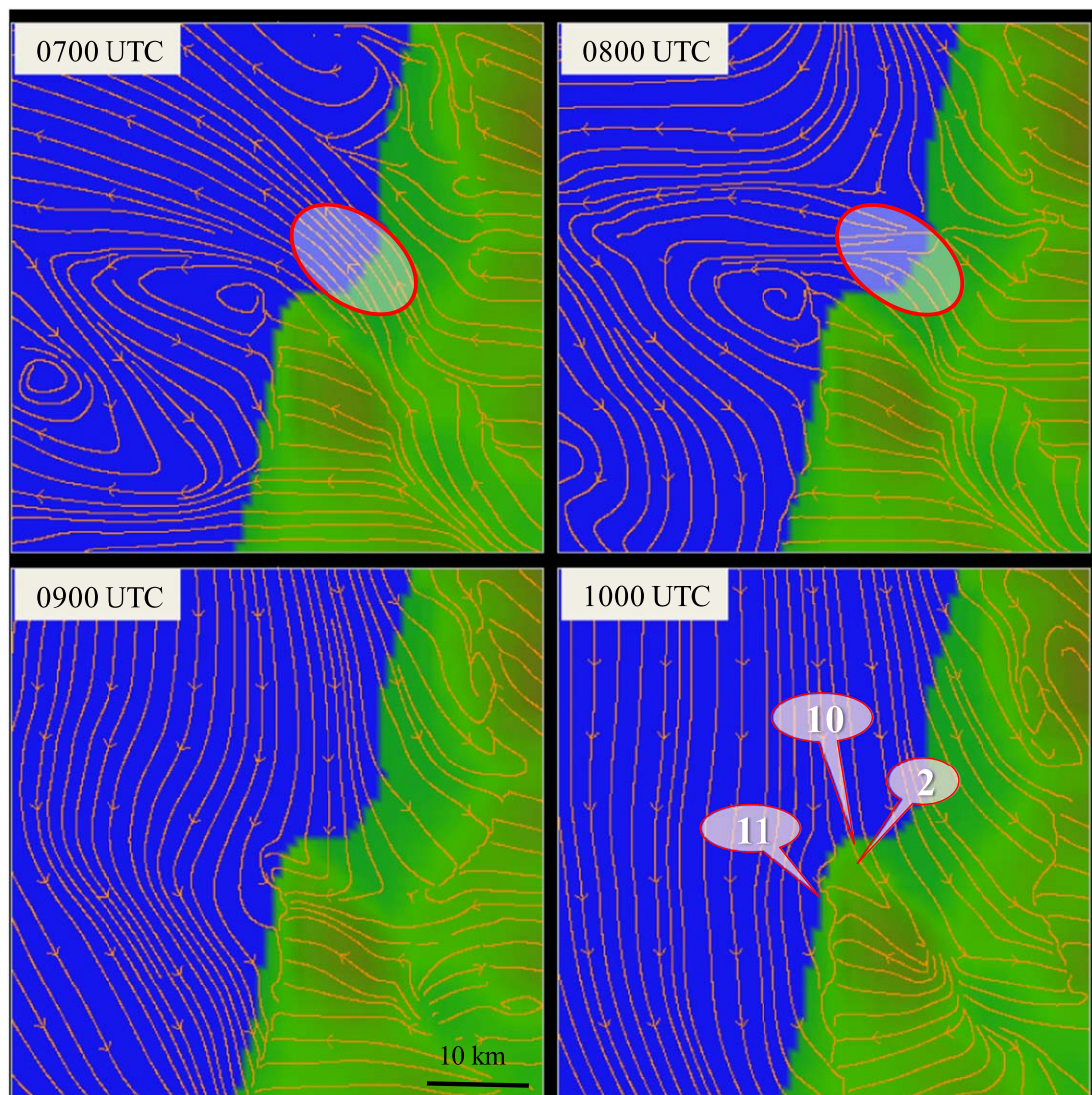


Figure 3. Simulated morning surface flow over Haifa region, where the arrow heads represent the flow direction. Wake circulation cell of 10–20 km is seen offshore at 0700 and 0800 UTC, and is totally destroyed by 1000 UTC. From 0700 to 0800 the flow at the bay changes by 90°, by 1000 UTC all of the coastal flow is northerly. Approximate locations of sites 2, 10, 11 are marked on the last frame.

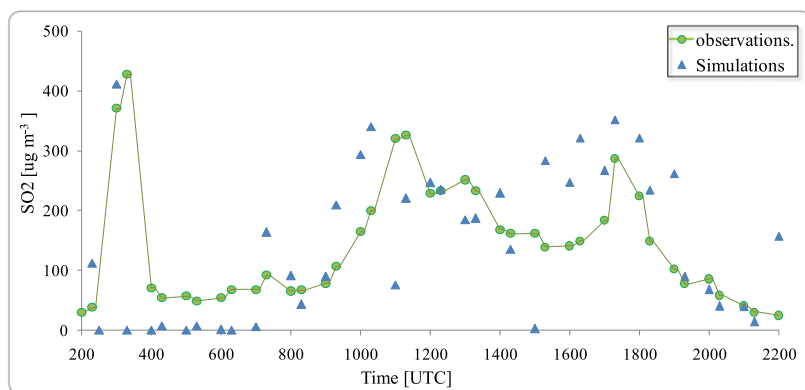
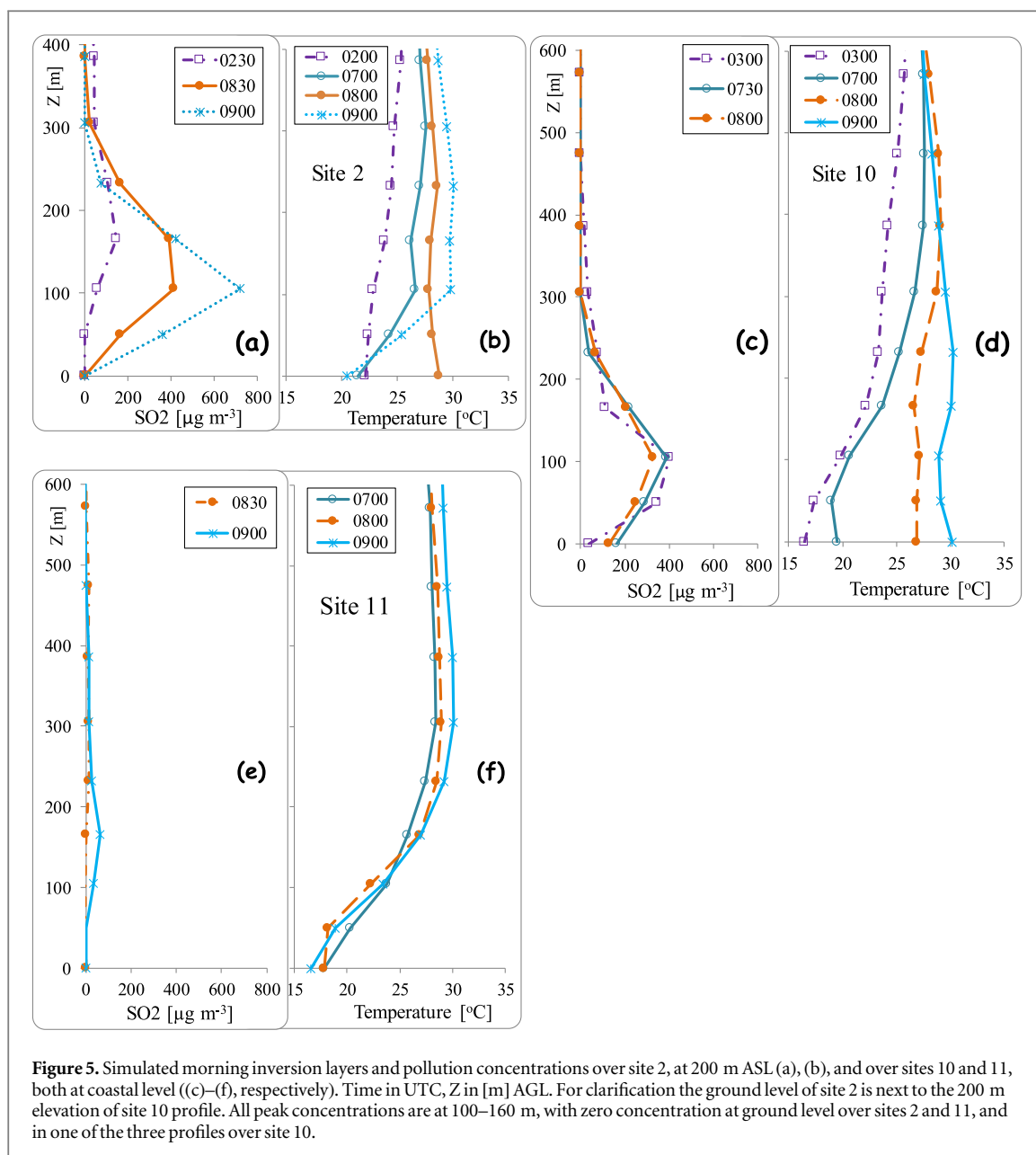


Figure 4. Comparison between simulated and observed maximum half-hourly concentrations of SO₂, at six ground stations (1, 3, 5, 7, 8, 9) (circles) and eight simulation receptors (1, 3, 4, 5, 7, 8, 9, 16) (triangles).



inversion and the pollution dispersion or accumulation beneath or within the layer, is of relevance for pollution dispersion. See elaboration in the supplementary material. Next (section 3.3), two cases are analyzed.

3.3. Pollutants near-surface concentration profiles

In the following sections vertical concentration profiles are addressed, with a focus on spatial variation. In many profiles we found zero (observed and simulated) concentration at ground level while high concentration values were found at 100–400 m AGL. This finding significantly differ from other studies which showed constant or decreasing values with elevation in the PBL (e.g. Li *et al* 2018, Sajani *et al* 2018). The nature of the emission sources may partially provide an explanation for the differences, where in this study we simulated high sources (stacks) while some of the other studies look at ground level sources. The scope of this paper does not allow presenting a thorough analysis of all sites, hence examples are presented and discussed in sections 3.3.1, 3.3.2.

3.3.1. Case A: morning thermal profiles over the coast

The three coastal sites 2, 10, 11 (figures 1, 3) are about 2 km apart. While sites 10 and 11 are close to sea level, site 2 is on Mt. Carmel at about 200 m ASL. Morning thermal profiles over these sites showed significant inversion layers, based at ground level or at 50–100 m AGL (figures 5(b), (d), (f)). The ground level temperature at the coastal site 10 is in the range of 15 °C–30 °C (figure 5(d)), while at the elevated site 2 it is 20 °C–29 °C (figure 5(b)), and at site 11 only 17 °C–18 °C (figure 5(f)). The inversion layers over the three sites are as deep as

Table 1. Dominating sites in seven sub periods along the case study. Deviation between simulated and observed sites is denoted as downwind, horizontal (sideways) and/or vertical (topographically higher or lower site).

Time [UTC]	Site (obs.)	Site (model)	Deviation
0200–0500	5	7	Horizontal and vertical
0500–0900	9	4	Downwind
0900–1300	8	16	Horizontal
1300–1430	8	8	Identical
1430–1900	8	5, 1	Horizontal
1900–1930	8	9	Horizontal
1930–2200	5	5, 16 + 8	Horizontal and vertical

300–400 m, and all peak concentrations are within the inversion levels, besides the peak at 0900 UTC (figure 5(a)) having its maximum at the top of the ground-based inversion. The concentration profiles over sites 2 and 11 show zero at the surface. The patterns in figure 5 suggest some terrain-following features of the thermal layers. Focusing on the 0900 UTC profiles one may see, that the highest peak is found at 100 m above site 2 (figure 5(a)), a much smaller peak at 150 m above site 10 (figure 5(c)), and no peak over site 11 (figure 5(e)). A close examination of the simulated flows at 100 m AGL showed a local circulation over site 2 with a northerly component from the zone of the emission sources, and a northerly flow over the coastal sites 10 and 11 (flow from the sea). However, over site 11 there is also a (north-easterly) component of a flow from the ridge top, which may explain the source origin for the small peak in figure 5(e). Also, as suggested in section 3.2.1 above, circulation cells over the edge of the ridge and into the sea, might have lead to the high concentrations over sites 2 and 10. After 0900 the emitted elevated plumes changed direction with the near-surface north-westerly flow. At the same time, the surface and near-surface levels above site 2 cleared out when the pollutants were transported towards site 16. There, high concentrations were built at the surface (see table 1) and even higher concentrations occurred at near-surface levels (not shown).

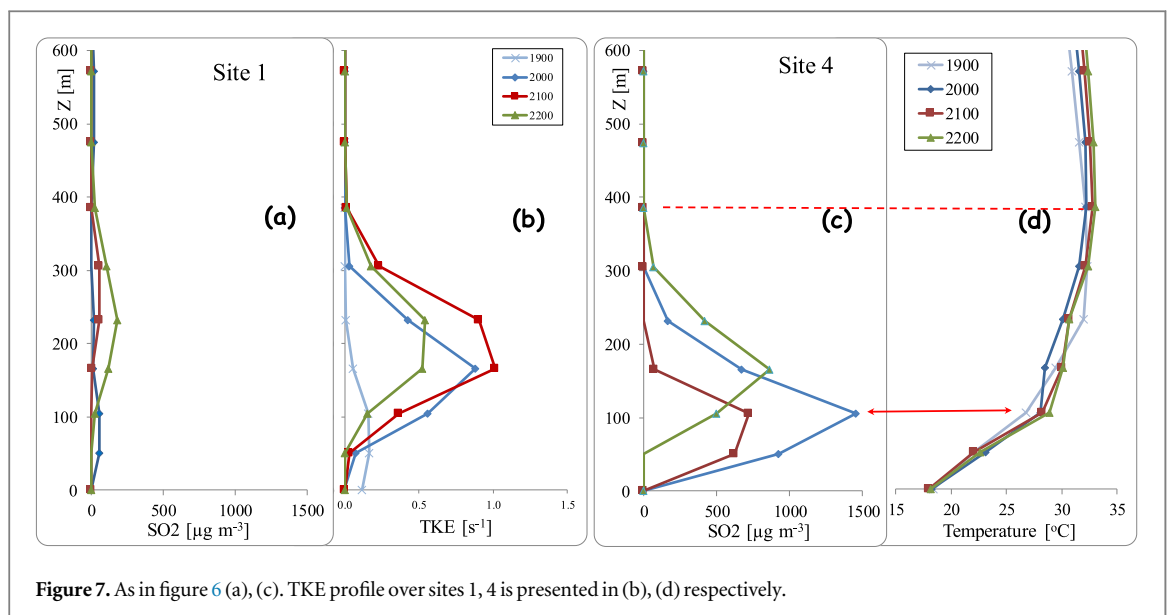
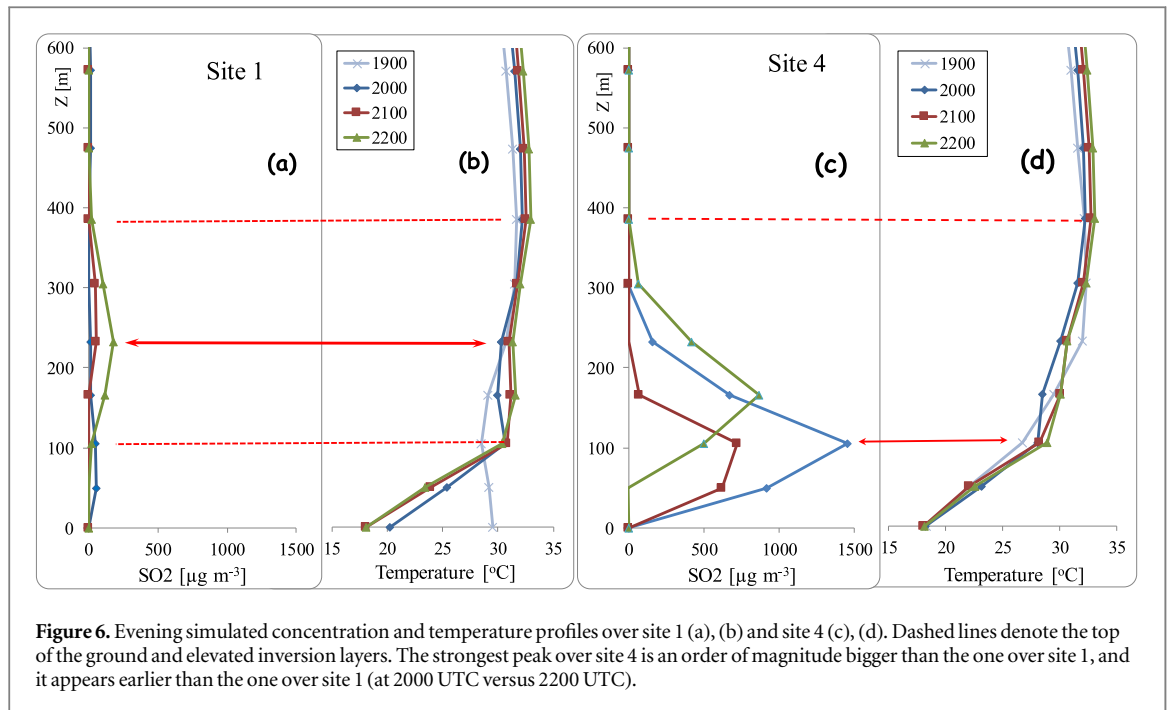
3.3.2. Case B—*evening profiles over the bay*

Sites 1 and 4 (as in figure 1) are located at about sea level, ~ 2.5 km apart each other. While site 1 is in an industrial area, site 4 is at the waterfront. Evening profiles over these two sites show no pollution at ground-level, yet they present a significant concentration at near surface elevated levels, with an order of magnitude difference between the sites (figure 6). Temperature profiles over both sites present a total of 400 m inversion depth, based on top of a very strong ground inversion. Since the inversion layers over both sites have similar dimensions, evidently, the temperature behavior (and wind, not shown) alone cannot explain the order-of-magnitude difference between the two sites. A further investigation revealed a TKE fit with the concentration pattern: the TKE over site 1 is five to ten times stronger than over site 4, which may explain the 10-fold lower concentrations over site 1, with respect to site 4. The TKE values over site 1 are within the scale of midday values, and may be the major reason for the strong suppression of the pollutant concentrations there. TKE pattern suggests a shallower ABL over site 4 compared to site 1 (figures 7(d) versus (b)), an additional parameter which also supports the formation of higher concentrations. Note, that in this case TKE is negligible at ground level while it is significant at elevated levels.

4. Conclusions

Danger may come from the least expected direction, as for instance from the ‘dead zone’ in a car’s mirror. Therefore, when it comes to strong pollution, it is most important to reduce the uncertainty as much as possible, and gain the best information on the mechanism and pattern. Analysis of adjacent vertical profiles of pollution showed numerous occurrences where no pollutant was observed or modeled at ground level, while high concentrations were found at a nearby site and/or at near-surface elevated levels, such outstanding cases were discussed above. This finding highlights the importance of gaining knowledge of near-surface elevated pollution, which is often not addressed in surface pollution studies.

High variability of pollution concentrations was found between adjacent sites, both at ground and at elevated layers, emphasizing the strong uncertainty of the pollutants dispersion in the study domain, with its most complex features. We presented local circulation cells over non-monitored sites, which were associated with high concentrations (section 3.3). An inverse relation between TKE and concentration peaks was found in elevated levels over adjacent sites, where weak TKE was associated with an order-of-magnitude higher



concentrations at elevated levels over one site, compared to the nearby site. The day-lasting deep inversion structure along the event in this study, had an impact on the formation of high concentrations, both at ground and elevated levels.

The simulated thermal profiles revealed multi-inversion structures, which agree with earlier observations over the region. An attempt to find (co)relation between the thermal profiles and the vertical structure of the pollution concentrations showed that persistent low-level inversions were associated with high pollutant concentrations close to the ground and at near surface elevated levels. However, higher vertical resolution is required, in order to explore the finer structures of the inversions, and their association with the pollution dynamics and patterns.

Results of this study highlight the importance of gaining a better understanding of the near-surface elevated layers as potential and unexpected pollution sources to the ground level. It is suggested that further modeling efforts with advanced models should be used to elaborate and further explore near-surface elevated pollution layers and their impact and interaction with surface layer. Remote sensing technology may also add useful spatial information of pollution dispersion near and over the local topography, and support the simulation effort. As expected, simulation results in this study illustrate the limits of even highly dense ground monitoring to indicate

occasional air pollution episodes: they may either miss concentration peaks or even totally miss the existence of air pollution plumes, when the plumes are slightly shifted from the monitoring station or above.

In summary, the near-surface steep vertical gradient of pollution as indicated here is associated with a combination of deep inversion (or multi-inversion), vertical circulation due to topography or synoptic flow, and small scale circulation induced by the complex topography.

Acknowledgments

This paper is dedicated to the late Prof. Yitzhak Mahrer, a dear advisor, teacher, colleague, friend, a unique atmospheric modeler and researcher, who passed away Sept. 2017. More details can be found at the BAMS obituary (July 2018). Prof. Mahrer was one of RAMS developers, and he participated in the early stages of this work.

The authors thank Haifa Towns Association for the Environment Protection and the Air Monitoring division in the Ministry of the Environment Protection, for their monitoring data.

This work was partly supported by the IAEC-Pazi Foundation.

ORCID iDs

Nitsa Haikin  <https://orcid.org/0000-0002-9213-1918>

Pinhas Alpert  <https://orcid.org/0000-0001-7179-6673>

References

- Alper-Siman-Tov D, Peleg M, Matveev V, Mahrer Y, Seter I and Luria M 1997 Recirculation of polluted air masses over the east Mediterranean coast *Atmos. Environ.* **31** 1444–8
- Alpert P, Osetinsky I, Ziv B and Shafir H 2004 A new seasons definition based on the classified daily synoptic systems: an example for the Eastern Mediterranean *Intern. J. of Climatol.* **24** 1013–21
- Astitha M, Kallos G and Katsafados P 2008 Air pollution modeling in the Mediterranean region: analysis and forecasting of episodes *Atmos. Res.* **89** 358–64
- Balanzino A and Trini Castelli S 2018 Numerical experiments with RAMS model in highly complex terrain *Environ. Fluid Mech.* **18** 357–81
- Cotton W R *et al* 2003 RAMS 2001: current status and future directions *Meteorol. Atmos. Phys.* **82** 5–29
- Doron E and Kinrot A 1989 Numerical simulation of worst SO₂ pollution episodes in Haifa Bay and Mount Carmel area *IV Int. Conf. on Environmental Quality and Ecosystem Stability (Jerusalem, Israel, 4–8 June 1989)*
- Eitan O, Yuval, Barchana M, Dubnov J, Linn S, Carmeli Y and Broday D M 2010 Spatial analysis of air pollution and cancer rates in Haifa Bay, Israel *Sci. Total Environ.* **408** 4429–39
- Garty J, Weissman L, Cohen Y, Karnieli A and Orlovsky L 2001 Transplanted lichens in and around the Mount Carmel national park and the Haifa Bay industrial region in Israel: physiological and chemical responses *Environ. Res.* **85** 159–76
- Goren A I, Hellman S, Brenner S, Egoz N and Rishpon S 1990 Prevalence of respiratory conditions among schoolchildren exposed to different levels of air pollutants in the Haifa Bay area, Israel *Environ Health Persp* **89** 225–31
- Grell G A, Emeis S, Stockwell W R, Schoenemeyer T, Forkel R, Michalakes J, Knoche R and Seidl W 2000 Application of a multiscale, coupled MM5/chemistry model to the complex terrain of the VOTALP Valley Campaign *Atmos. Environ.* **34** 1435–53
- Haikin N, Galanti E, Reisin T G, Mahrer Y and Alpert P 2015 Inner structure of atmospheric inversion layers over Haifa Bay in the Eastern Mediterranean *Boundary-Layer Meteorol* **156** 471–87
- Hobbs P V 2000 *Introduction to Atmospheric Chemistry* (Cambridge: Cambridge University Press) pp 262
- Jazcilevich A D, Garcia A R and Ruiz-Suarez L G 2003 A study of air flow patterns affecting pollutant concentrations in the Central Region of Mexico *Atmos. Environ.* **37** 183–93
- Kallos G, Kassomenos P and Pielke R A 1993 Synoptic and mesoscale weather conditions during air pollution episodes in Athens, Greece *Bound-Lay Meteorol* **62** 163–84
- Kalnay E *et al* 1996 The NCEP/NCAR 40-year reanalysis project *Bull Amer Meteorol Soc* **77** 437–70
- Kerr G H and Waugh D W 2018 Connections between summer air pollution and stagnation *Environ. Res. Lett.* **13** 084001
- Kotroni V, Kallos G, Lagouvardos K, Varinou M and Walko R 1999 Numerical simulations of the meteorological and dispersion conditions during an air pollution episode over Athens, Greece *J. Appl. Meteorol.* **38** 432–47
- Lang M N, Gohm A and Wagner J S 2015 The impact of embedded valleys on daytime pollution transport over a mountain range *Atmos. Chem. Phys.* **15** 11981–98
- Levy I, Dayan U and Mahrer Y 2009 Coastal and synoptic recirculation affecting air pollutants dispersion: a numerical study *Atmos. Environ.* **43** 1991–9
- Li X-B, Wang D S, Lu Q C, Peng Z R and Wang Z Y 2018 Investigating vertical distribution patterns of lower tropospheric PM_{2.5} using unmanned aerial vehicle measurements *Atmos. Environ.* **173** 62–71
- Mahrer Y and Pielke R A 1977 The effects of topography on sea and land breezes in a two-dimensional numerical model *Mon. Weather Rev.* **105** 1151–62
- Mamane Y and Gottlieb J 1995 Ten years of precipitation chemistry in Haifa, Israel *Water Air Soil Poll* **82** 549–58
- Mamane Y and Mehler M 1987 On the nature of nitrate particles in a coastal urban area *Atmos. Environ.* **21** 1989–94
- Matthaios V N, Triantafyllou A G and Koutrakis P 2017 PM₁₀ episodes in Greece: local sources versus long-range transport—observations and model simulations *J. Air Waste Manage. Assoc.* **67** 105–26
- Matthaios V N, Triantafyllou A G, Garas S, Krestou A and Leivaditou E 2017b Interactions between complicated flow-dispersion patterns *Meteorol Atmos Phys (2017)* **129** 425–39
- McLagan D S, Hussain B A, Huang H, Lei Y D, Wania F and JMitchell C P 2018 Identifying and evaluating urban mercury emission sources through passive sampler-based mapping of atmospheric concentrations *Environ. Res. Lett.* **13** 074008

- Paz S, Linn S, Portnov B A, Lazimi A, Futerman B and Barchana M 2009 Non-Hodgkin Lymphoma (NHL) linkage with residence near heavy road—a case study from Haifa Bay, Israel *Health Place* **15** 636–41
- Perez-Landa G, Ciaia P, Gangoiti G, Palau J L, Carrara A, Gioli B, Miglietta F, Schumacher M, Millán M M and Sanz M J 2007 Mesoscale circulations over complex terrain in the Valencia Coastal Region, Spain: II. Modeling CO₂ transport using idealized surface fluxes *Atmos. Chem. Phys.* **7** 1851–68
- Pielke R A, Cotton C J, Walko R L, Tremback C J, Lyons W A, Grasso L D, Nicholls M E, McNider R T, Segal M and Mahrer Y 1983 The use of a mesoscale numerical model for evaluation of pollutant transport and diffusion in coastal regions and over irregular terrain *Bull. Am. Meteorol. Soc.* **64** 243–9
- Reuten C, Steyn D G, Strawbridge K B and Bovis P 2004 Observations of the relations between upslope flows and convective boundary layer in steep terrain *Bound-Lay Meteorol* **116** 37–61
- Ritter M, Muller M D, Tsai M Y and Parlow E 2013 Air pollution modeling over very complex terrain: an evaluation of WRF-Chem over Switzerland for two 1-year periods *Atmos. Res.* **132–133** 209–22
- Sajani S Z *et al* 2018 Vertical variation of PM_{2.5} mass and chemical composition, particle size distribution, NO₂, and BTEX at a high rise building *Environ Poll* **235** 339–49
- Schmitz R 2005 Modelling of air pollution dispersion in Santiago de Chile *Atmos. Environ.* **39** 2035–47
- Soriano C, Baldasano J M, Buttler W T and Moore K R 2001 Circulatory patterns of air pollution within the Barcelona air basin in summertime situation: LIDAR and numerical approaches *Bound-Lay Meteorol* **98** 33–55
- Stull R 1988 *An Introduction to Boundary Layer Meteorology* (Dordrecht: Kluwer Academic Publishers) p 666
- Valverde V, Pay M T and Baldasano J M 2016 A model-based analysis of SO₂ and NO₂ dynamics from coal-fired power plants under representative synoptic circulation types over the Iberian Peninsula *Sci. Total Environ.* **541** 701–13
- Wagner J S, Gohm A and Rotach M W 2015 The impact of valley geometry on daytime thermally driven flows and vertical transport processes *QJR Meteorol Soc* **141** 1780–94
- Walko R L, Tremback C J and Bell M J 2001 *HYPACT Version 1.2.0 User's Guide* (PO Box 466, Fort Collins, CO: ASTER Division Mission Research Corporation)
- Yuval and Broday D M 2006 High-resolution spatial patterns of long-term mean concentrations of air pollutants in Haifa Bay area *Atmos. Environ.* **40** 3653–64